

Computed Radiography Imaging Based on High-Density 670 nm VCSEL Arrays

Matthew M. Dummer, Klein Johnson, Mikael Witte, William K. Hogan,
and Mary Hibbs Brenner

Vixar, 15350 25th Ave N., Plymouth MN, USA

ABSTRACT

We present a new laser scanning technology based on one-dimensional VCSEL arrays. A device that uses on this concept has been developed for computed radiography applications. The scanner consists of a 1-inch linear array containing 240 red lasers. High-speed laser drivers and a GRIN lens array are incorporated to create an ultra-compact scanner with no moving parts. This configuration has been used to successfully digitize x-ray images. The approach potentially offers higher throughput and resolution than current CR readers, while improving overall compactness and mechanical stability.

Keywords: Computed Radiography, Medical Imaging, VCSEL, Semiconductor Laser

1. INTRODUCTION

Although vertical cavity surface emitting lasers (VCSELs) have traditionally found their place in high-speed communication links, the recent advancements of VCSELs emitting in the visible spectrum has sparked interest for new applications in scanning and imaging. Compared to other lasers, VCSELs have many advantageous characteristics including compact size, low power requirements, low cost, and high reliability. VCSELs also offer the unique ability to be fabricated in one- or two-dimensional arrays, making it possible for multiple VCSELs on a single chip to perform the same function as a mechanically scanned beam. One such application is computed radiography (CR), which provides an efficient solution for digitizing and electronically storing x-ray images. In this work, we demonstrate a 1-inch prototype CR scanner based on high-density VCSEL arrays. The device is capable of generating very fast scans with no moving parts, and has the potential to increase throughput, stability, and image quality. In this paper, we discuss the design and performance of this scanner and demonstrate X-ray image acquisition with resolution exceeding 5 line pairs per millimeter (lp/mm).

2. COMPUTED RADIOGRAPHY BACKGROUND

Computed radiography systems have provided a versatile and cost effective technique for digitization of medical x-ray images for over twenty five years.¹ The key component of CR is a specialized phosphor screen, which replaces traditional film for capturing an image. When exposed to x-ray energy, electrons in the phosphor crystal lattice are excited and become trapped at a higher energy, where they can remain for several hours before eventually decaying to their ground state.² Additionally, the phosphor screen is photostimulable such that subsequent exposure to a specific optical energy can trigger relaxation of the trapped electrons and release corresponding photons at a new emission wavelength. Therefore, by scanning a laser beam over an exposed screen and detecting the emitted energy at each location, the image stored in the phosphor can be recovered and converted to a digital format. The excitation wavelength range for most commonly used phosphors is between 550 and 700 nm (red), while the stimulated emission wavelength is near 400 nm (blue).³ Most CR scanners therefore make use of a HeNe, or diode laser emitting in the 600 nm range as the photostimulation source. A rotating mirror, as well as additional beam shaping optics are incorporated to create a "flying spot scanner" which rasters a beam over the surface of the phosphor plate. Meanwhile, the plate is also slowly moving orthogonal to the beam scan direction to acquire the full two dimensional image. The hardware needed to deflect the beam, and the optical path length required to prevent spot-size distortion are two of the biggest factors affecting the cost and overall size of CR scanners today. For this reason, other scanning technologies are currently being developed.⁴

Further author information: (Send correspondence to Matthew Dummer)
E-mail: mdummer@vixarinc.com, Telephone: (763) 746-8045

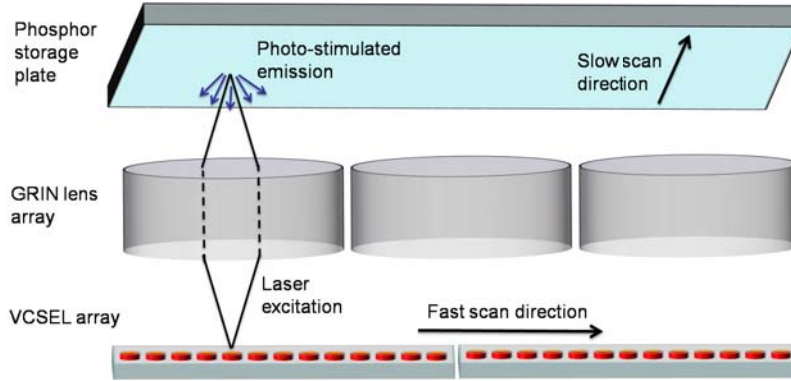


Figure 1. Conceptual diagram of the compact CR scanner based on 1-D VCSEL arrays

3. VCSEL ARRAY SCANNER

This work proposes an alternative to the flying spot scanner based on high-density VCSEL arrays. The use of VCSEL technology allows multiple emitters to be fabricated on a single chip in a wafer scale process. Using this process, lasers in the array can be spaced close enough to have a one-to-one correspondence with the pixels in the fast-scan direction. A graded index (GRIN) lens array is added above the VCSELs, to focus the light onto the phosphor plate. A diagram of this type of scanner is depicted in Fig. 1. By turning on and off each laser sequentially, a scanning beam is created which is functionally analogous to a flying spot scanner. However, the VCSEL approach results in an ultra-short path length with minimal additional optics and no moving parts. Similar multi-element scanners have already been implemented in printers using light emitting diodes (LEDs).⁵ However, a scanner using a high-density laser array has never been demonstrated before now. This is mainly due to the significant increase in fabrication complexity of lasers compared with LEDs, and the associated lower device yield.

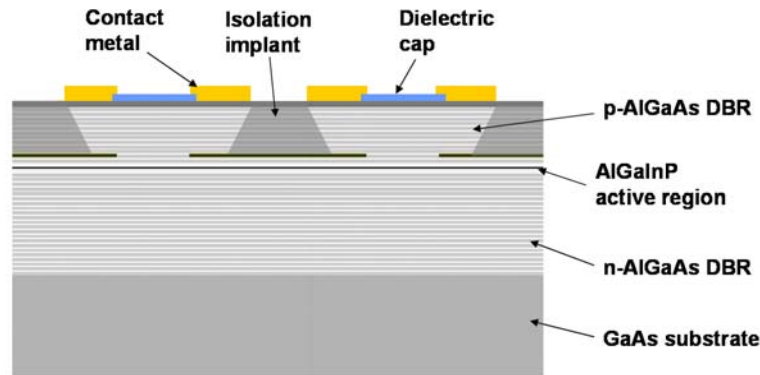


Figure 2. Cross section of VCSEL array structure

4. VCSEL FABRICATION AND ARRAY ASSEMBLY

The laser arrays designed and fabricated for this work are similar to high-power 670 nm VCSELs previously published.⁶ A cross sectional diagram of two VCSELs in an array is shown in Fig. 2. The devices are epitaxially grown on GaAs substrates using metalorganic chemical vapor deposition (MOCVD). The layer structure consists of top and bottom AlGaAs distributed Bragg reflector (DBR) mirror stacks surrounding an AlGaInP multi-quantum-well (MQW) laser active region. Patterning and metallization is performed using standard photolithographic and semiconductor processing techniques. Individual lasers within the arrays are electrically isolated by ion implantation of the upper (p-type) material. The diameter of the VCSEL emitters, including

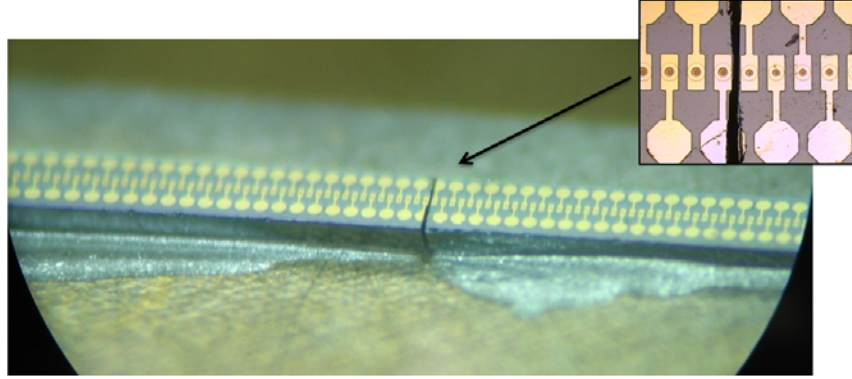


Figure 3. Placement of individual VCSEL die to achieve a 1-D super-array. VCSELs maintain a $50 \mu\text{m}$ pitch across chip boundaries.

metal ring contacts can be made as narrow as $20 \mu\text{m}$. However, the space required for metal interconnects and wirebonding pads necessitates at least a $50 \mu\text{m}$ spacing for a one dimensional array. This corresponds to a maximum image resolution of 500 dpi.

Typical CR scanners are designed to accommodate phosphor plates as wide as 18 inches. However, due to the small size of GaAs substrates as well as yield considerations, it is not possible to make a single-chip VCSEL array for the full scanner width. Instead, many die must be cascaded end-to-end on a circuit board to create a “super array” of the desired length. Choosing the number of VCSELs per array is a trade off between packaging complexity and yield. Smaller die require more chips to be placed to achieve the desired super array, while larger die increase the probability of a single VCSEL failure. Furthermore, for very long arrays, the long and narrow footprint makes handling of the die cumbersome. In this work, array sizes have been limited to at most 96 VCSELs, resulting in a chip length of 5 mm. Precise placement using accurate die bonding tools allows the array spacing to remain continuous across the chip boundaries, within micron tolerances. Figure 3 depicts a photograph of a VCSEL super array which maintains a $50 \mu\text{m}$ pitch chip-to-chip.

5. ARRAY CHARACTERIZATION

Replacing a single-laser scanner with a multi-VCSEL array requires a high degree of uniformity to maintain a constant optical power over the image field. Individual arrays must be tested at the wafer level before assembly of the super-arrays to screen for non-uniformity. Figure 4(a) shows the typical operating characteristics for a laser array with 64 VCSELs. The devices exhibit moderate differences in threshold current, with average laser turn-on occurring near 5 mA. The power variation at low current is due to thermal lensing, a temperature dependent index shift that results in modal fluctuations.⁷ However, at higher currents the operating power is much more uniform across the array. For example, at 14 mA the power variation across the array is less than 10 percent. Also, the electrical characteristic (voltage versus current) for every VCSEL is nearly identical. The power distribution of multiple VCSEL array die has also been examined, as shown in Figure 4(b). The histogram shows the maximum measured power from 20 die, of which each element meets a minimum specification of 5.5 mW. The average maximum power for all 1280 lasers is 6.0 mW, with a standard deviation of 0.21 mW. While not insignificant, this amount of non-uniformity can be easily compensated for, either by hardware or software implementation.

Another source of non-uniformity in the scanner is due to the GRIN lens array used to focus each beam onto the phosphor. The lenses used in this work are commercially available close-packed GRIN-rod lenses with a diameter of 0.9 mm. The large discrepancy between the lens pitch and the VCSEL pitch causes misalignment across the array, with some VCSELs falling directly between two lenses. This misalignment has been studied to determine the effect on the output power. As shown in Fig. 5(a), a periodic variation in output power occurs with respect to lens position. The maximum power variation is measured to be 0.3 dB, and the average insertion loss of the GRIN lens is 1.4 dB. The output spot size of a single VCSEL beam has also been measured at the

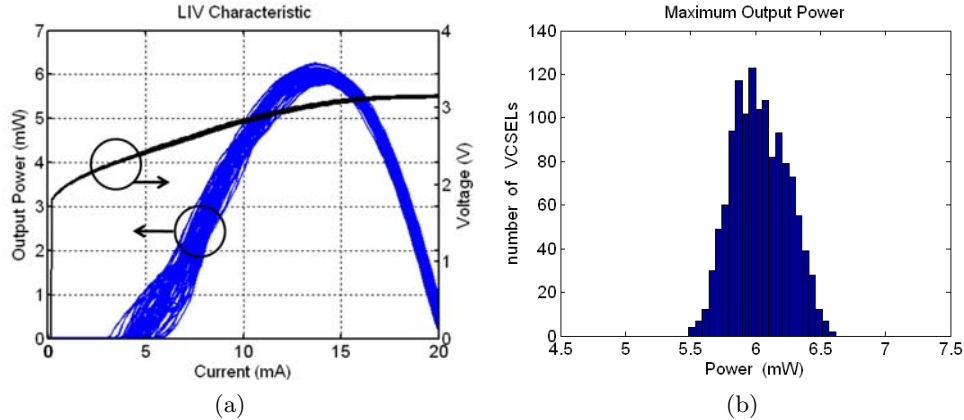


Figure 4. (a) Light output versus current and voltage (LIV) for individual lasers in a 1x64 670 nm VCSEL array. (b) Measured maximum output power distribution for twenty 1x64 VCSEL arrays

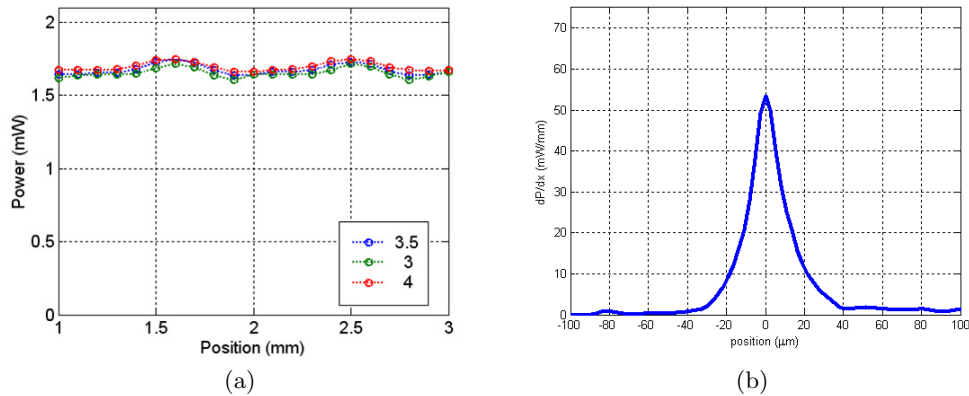


Figure 5. (a) Measured uniformity of GRIN lens array as a function of position along the scanning direction. The three curves represent three different focal lengths given in mm. (b) Beam profile of VCSEL at the GRIN lens focal length of 3.46 mm)

image plane of the lens, shown in Fig 5(b). The full width of the beam is less than $40 \mu\text{m}$, which is sufficient for achieving the maximum resolution of the scanner.

6. SCANNER DESIGN AND IMAGING EXPERIMENTS

Using the components described above, a one-inch-wide laser scanner has been fabricated and tested. The laser array consists of five 1x96 VCSEL die. The die are placed end-to-end on a Kapton flex circuit with the GRIN lens assembly mounted above (Fig. 6). To simplify packaging of this prototype, a 200 hundred micron gap was allowed between the die. Wirebonds are made from each of the VCSELs to interconnect traces on the flexible circuit board. The dense spacing of the VCSELs requires bondpads to be alternately fanned out to either side of the array. However, for simplicity only one side of bondpads is wirebonded to the flex circuit, resulting in half the number of active lasers. This leads to an effective VCSEL pitch of $100 \mu\text{m}$. The flexible interconnect traces are connected to a laser-driver circuit board, designed to execute the scanning function for the array. The driver board relies on multiple arrayed current sources, which are cascaded together through a series shift registers to address each pixel sequentially. Additional logic is included to set the dwell time of each pixel and the pattern for triggering each new line.

Imaging experiments have been performed using an adapted commercial Carestream Healthcare CR system. The original flying spot scanner was removed and the VCSEL scanner was retrofitted within the light collection

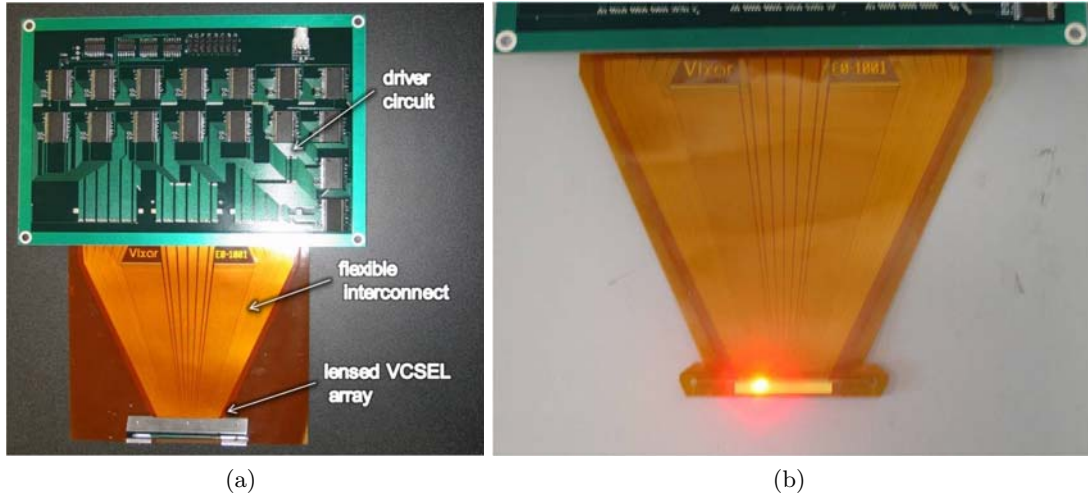


Figure 6. (a) Assembled 1-inch laser scanner. (b) Photograph of active VCSEL array.

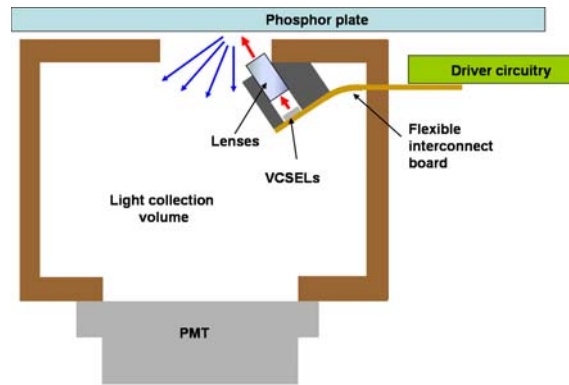


Figure 7. Cross section of CR scanner and light collection assembly

assembly. A basic diagram of the experimental setup is depicted in Fig. 7. The scanner head was positioned such that the laser spot was aimed through a slit in the light collector and focused onto the phosphor plate. Stimulated emission from the phosphor was collected by the reflective assembly and detected by a photomultiplier tube (PMT). The resulting electrical signal was digitized and stored. A master clock signal was used to synchronize the laser driver board and detection system to properly reconstruct the X-ray image.

To test the VCSEL array scanner, a phosphor screen was first exposed with a resolution target. A scan of the screen was then taken using a 5 mW pulse power with a 1 μ s dwell time at each pixel location. The acquired raw image is shown in Fig. 8, which clearly reconstructs the features of the target. In this case, x and y represent the slow and fast scan direction, respectively. Four white horizontal lines appear in the fast scan y direction because of the 2-pixel gap introduced in the placement of the VCSEL die. However, these could be eliminated with continuous VCSEL spacing as shown in Fig. 3. Other variations in the intensity of the image in the y direction are a result of VCSEL non-uniformity issues described above. Current efforts to improve VCSEL performance as well as better software calibration should be able to reduce this effect.

The acquired image has been analyzed to determine the scanner's resolution. Figure 9 shows the lower portion of the same image after contrast enhancement. The normalized intensity at a fixed y position is also plotted to show the modulation intensity. Features sizes varying from 2 lp/mm to 5 lp/mm are shown from left to right. Although all lines are resolvable, the modulation transfer function is noticeably reduced to 50 percent at 5 lp/mm.

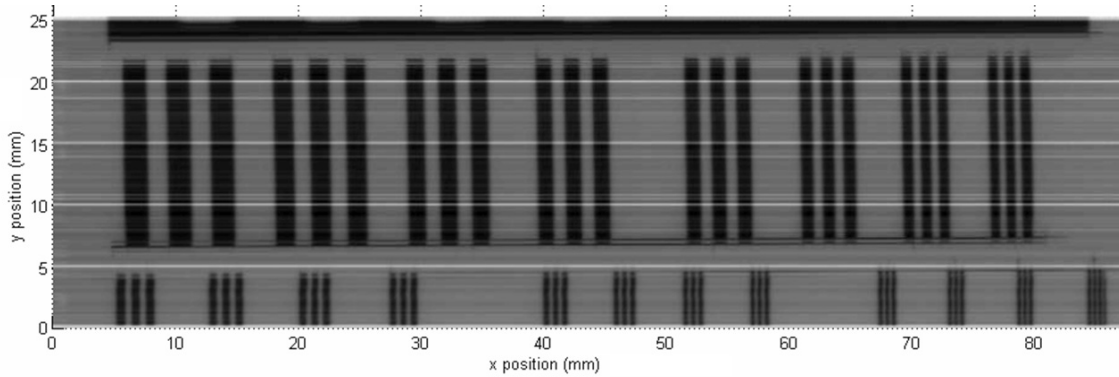


Figure 8. Acquired raw X-ray image using VCSEL scanner

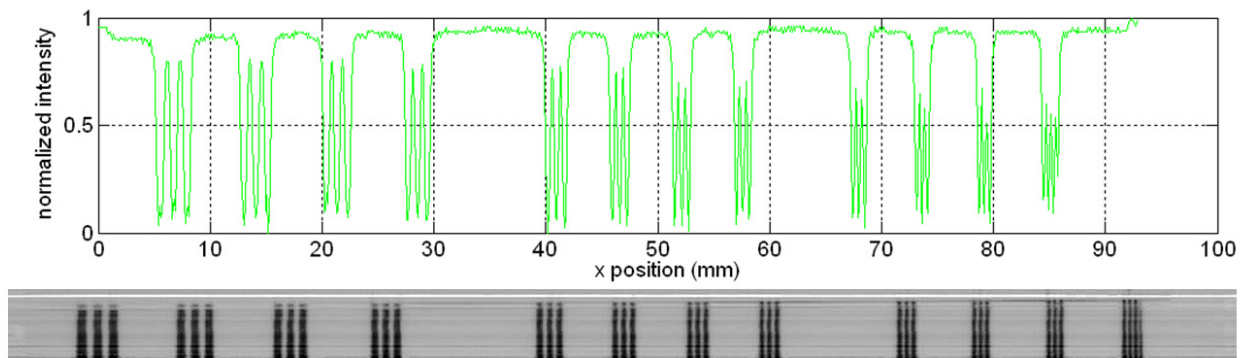


Figure 9. (lower) Smaller features on resolution target after image contrast enhancement. (upper) Plot of normalized image intensity at $y = 2\text{mm}$

7. CONCLUSION

We have presented a new compact laser scanner for CR based on integrated VCSEL arrays. A proof-of-concept device has been assembled and used to digitize actual X-ray images. Preliminary testing shows that the scanner is capable of resolution of at least 5 lp/mm. Although this device was only one inch long using a $100\ \mu\text{m}$ laser pitch, the array is easily scalable to much longer scan lengths and higher VCSEL density. Future work is focused on improving the VCSEL array uniformity, and packaging techniques. These improvements, along with optimized logic design to further reduce the size, will make the VCSEL scanner very attractive for future CR applications.

ACKNOWLEDGMENTS

This work has been performed with support from the National Institute of Health under SBIR grant number 1R43RR 025874-01. The authors would also like to acknowledge Carestream Healthcare for providing access to radiography equipment and their help in acquiring the X-ray images above.

REFERENCES

1. R. Schaetzing, R. Fasbender, and P. Kersten, "New high-speed scanning technique for computed radiography," *Medical Imaging 2002: Physics of Medical Imaging* **4682**(1), pp. 511–520, 2002.
2. A. Cowen, A. Davies, and S. Kengyelics, "Advances in computed radiography systems and their physical imaging characteristics," *Clinical Radiology* **62**(12), pp. 1132 – 1141, 2007.
3. J. A. Rowlands, "The physics of computed radiography," *Physics in Medicine and Biology* **47**(23), pp. R123–R166, 2002.

4. R. Schaetzing, "Computed radiography technology," *Samei E, Flynn MJ, eds*, pp. 7–22, 2003.
5. K. Tateishi and Y. Hoshino, "Electrophotographic Printer Using LED Array," *Industry Applications, IEEE Transactions on* **IA-19**, pp. 169–173, March 1983.
6. K. Johnson and M. Hibbs-Brenner, "High output power 670nm VCSELs," in *Proc. of the SPIE, Photonics West Symposium on Vertical Cavity Surface Emitting Lasers*, pp. 6484–04, 2007.
7. W. Nakwaski, "Thermal aspects of efficient operation of vertical-cavity surface-emitting lasers," *Optical and Quantum Electronics* **28**(4), pp. 335–352, 1996.